2021 43rd Annual International Conference of the
IEEE Engineering in Medicine & Biology Society (EMBC)
Oct 31 - Nov 4, 2021. Virtual Conference

Wireless Power Transmission with Uniform Power Delivery in the 3D Space of the Human Body using Resonators in Parallel

Reepa Saha, *Student Member, IEEE*, Bhadhan Roy Joy, *Student Member, IEEE*, and S. A. Mirbozorgi, *Member, IEEE*

***Abstract*—This paper presents a novel resonance-based multi-coil wireless power transmission (WPT) system for powering implantable devices inside the 3D space of the human body. This design consists of a power amplifier, a transmitter coil, a cluster of resonators in parallel configuration, and a receiver unit, working at 13.56 MHz (the FCC-approved ISM-band). The proposed cluster configuration of the resonators in parallel configuration guarantees homogenous electromagnetic fields and uniform wireless power distribution in the 3D space of the body. It localizes the transmitted power at the receiver location naturally by activating the resonators near the receiver. We have modeled the proposed inductive link and the human body with HFSS software to optimize the design and study the body's safety by evaluating the Specific Absorption Rate (SAR) level. The proposed WPT system is implemented, and the measured results show that the inductive link with multiple resonators in parallel configuration can continuously deliver power, >120 mW, wirelessly inside the 3D space of the human-torso with a power transfer efficiency (PTE) of 15%, uniformly. We have also extended the coverage area to the human forearm by paralleling resonators with the resonators in the central body. The power delivered to the load and PTE between the resonators on the forearm area are measured >90 mW and ~14%, respectively.**

***Index Terms*— Wireless Power Transmission, Multi-Coil Inductive Link, Parallel Resonators, Implanted Medical Device.**

I. Introduction

The wireless power transmission (WPT) technology, using inductive links, has been employed in numerous applications to transfer power for more than a century [1]. The WPT technology has been used to wirelessly power/charge portable battery-powered devices such as smartphones, industrial and biomedical sensors, electric-vehicles, etc. [2]. The inductive link technology is demonstrated as an excellent approach for sending sub-micro to several tens of milliwatts to implantable devices wirelessly, used for both small animals and humans, to avoid using bulky rechargeable batteries and frequent surgeries to replace them.

A variety of implants and head-mounted devices are developed for small animals to study the body's biology and neurology [3]. Such knowledge and technologies help develop human-specific medical implants, including vital sign monitoring sensors and devices, neural interfaces, retinal/cochlear implants, drug delivery implants, etc. [4]-[5]. Additionally, the WPT technology has the potential to revolutionize the modern medical treatment and diagnosis systems by facilitating the development of 1) tumor ablation devices, using a radio-frequency, microwave, laser, and high-intensity focused ultrasound energy for treating liver and kidney tumors, colon cancer, breast cancer, etc. [6], [7], and 2) endoscopy devices [8].

Improving power transfer efficiency of inductive links, extending the coverage area and distance, and increasing the power delivery (considering the safety issues) are the main objectives of the new and future WPT designs. 3-coil and 4-coil inductive link configurations have already been developed to address these objectives for different applications with different requirements [9]. Different configurations of multicoil transmitter arrays are proposed (including the switching approaches, floating resonators designs, parallel resonators designs, etc.) to increase the effective active area where a receiver unit can be located and received sufficient wireless power [2].

A system with resonators in parallel configuration has the capability of providing uniform PTE and power delivered to the load (PDL) over a large surface or in a large volume by unifying the electromagnetic field and its natural power localization property. This WPT configuration is developed for small animal wireless power cages (for long-term in-vivo experiments with freely moving animals) and smartphone charging platforms [2], [3].

This work extends the application of the parallel-resonator-based WPT configurations by introducing a novel multi-coil inductive link design for wirelessly powering implantable devices in the 3D space of the human body. Section II provides the design description and simulation results of the proposed resonators-based inductive link. Section III incorporates the experimental results, followed by the conclusion in Section IV.

II. Design Overview

A. Design Description

The conceptual schematic of the proposed multi-coil wireless power link is illustrated in Fig. 1a. The transmitter design consists of a Class E Power Amplifier (PA) powered by a battery, a transmitter (Tx) coil (L_1), and resonators in

Reepa Saha is a graduate student at the Electrical and Computing Engineering Department, University of Alabama at Birmingham, Birmingham, AL 35294 USA (email: reepa@uab.edu)

Bhadhan Roy Joy is a graduate student at the Department of Computer Science, University of Alabama at Birmingham, Birmingham, AL 35294 USA (email: bjoy@uabmc.edu)

S. Abdollah Mirbozorgi: Electrical and Computing Engineering Department, the University of Alabama at Birmingham, Birmingham, AL 35294 USA (phone: 205-934-8412; email: samir@uab.edu)

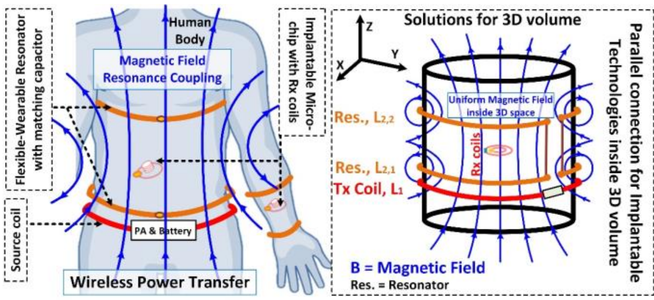

(a) (b)

Fig. 1. (a) Conceptual schematic of the proposed multi-coil parallel configuration for powering implants in the 3D space of the Human-body, and (b) the electromagnetic field pattern, generated by resonators in parallel configuration.

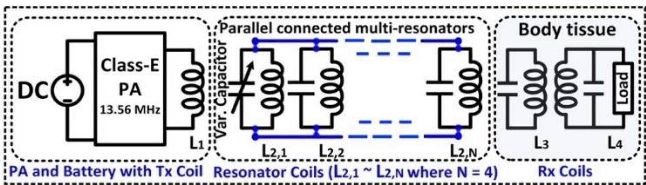

Fig. 2. The equivalent circuit model of the proposed 4-coil-based inductive link with N (here, N = 4) parallel resonators configuration, including transmitter coil (L_1), parallel connected resonator coils ($L_{2,1}$, $L_{2,2}$, $L_{2,3}$, and $L_{2,4}$), and receiver unit with load coil (L_4) and receiver resonator (L_3).

parallel configuration ($L_{2,i}$). Each resonator made of an inductor, L, and a capacitor, C (LC-Tank), and multiple resonators (in parallel configuration) made a cluster. The receiver, Rx, unit (implantable device) consists of a receiver resonator (L_3) and receiver load coil (L_4). The conceptual schematic of proposed parallel configuration of the resonators is shown in Fig. 1b, indicating the orientation of the generated electromagnetic field. The proposed cluster of the Tx unit generates uniform electromagnetic field in the 3D space of the human body. The cluster has only one variable capacitor for all the resonators in parallel configuration to fine-tune the resonance frequency of the entire inductive link at 13.56 MHz. The Tx coil, L_1, has a strong coupling with one resonator ($L_{2,1}$) in the cluster, and the number of the resonators (N) in the cluster is determined based on the required coverage area of the target application.

Fig. 2 shows the equivalent circuit model of the proposed system, indicating the cluster with N resonators. The main objectives of optimizing the Tx coil and cluster design are 1) maximizing the power transfer efficiency, PTE, 2) maximizing the uniformity of PTE/PDL across 3D space of the body, 3) minimizing the number of resonators in the cluster, and 4) minimizing the SAR across the body. The input optimization parameters are the human body size, the receiver's dimension and weight, specific target location of the receiver inside the body, required power level at the receiver, uniformity in 3D space or over the 2D surface, SAR safety considerations, and the Tx unit's flexibility considerations. The optimization outcomes are all coils parameters such as the number of turns, gaps between coils to determine cluster's coils locations, quality factors, coupling coefficients, and therefore maximum achievable efficiency (PTE) and power delivery to the load (PDL).

B. Optimization and Simulation Results

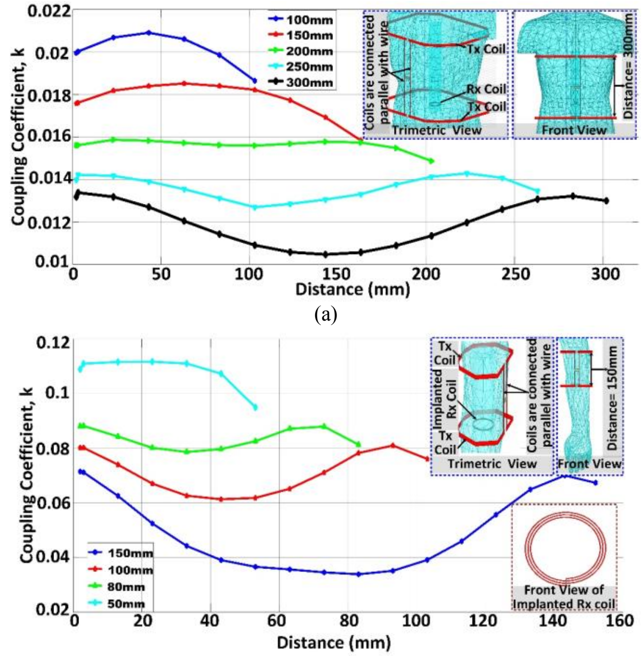

(a)

(b)

Fig. 3. The HFSS simulation results for finding the optimum distance between two resonators connected in parallel; the coupling coefficients as a function of distance for different gaps between the resonators in parallel configuration, located around (a) the human-chest and waist area, and (b) the human arm model. The insets show the HFSS models of the paralleled resonators and human body model.

When the Rx unit dimension is much smaller than the Tx coil (or Tx resonator/s), the design of the Tx unit is totally independent of the design of the Rx unit, which is the case in this work [10]. The optimum distance between Tx coil and its closest resonator of the cluster is not necessarily the smallest possible distance or maximum achievable coupling coefficient, k. The optimal value of k is proportional to the minimum values of the reflection coefficients, S_{11}, of the Tx coil, while it is coupled with resonator/s (or one resonator of the cluster in this work). The S_{11} can be calculated by (1),

$$S_{11} = \frac{Z_{11} - R_S}{Z_{11} + R_S}, \quad (1)$$

where Z_{11} is the impedance of Tx coil and R_s is the source resistance. Therefore, we can sweep the gap between the Tx coil and the first resonator ($L_{2,1}$, closest resonator to the Tx coil) to find the optimum gap and k, or minimum S_{11} in our simulation. The diameters (and shapes) of the Tx coil and the resonators are determined by the application requirements (body size). If more resonators are added/paralleled in cluster, the gap between the Tx and the first resonator might need to be changed to optimize the performance of the Tx unit regarding the PTE, PDL, SAR, etc. The optimum gaps between the resonators in parallel configuration can be determined considering the S_{11} level and uniformity of the PTE and PDL in the 3D spaces between them. The same procedure can be used to optimize the performance of the Rx unit (the size of and the gap between the receiver resonator and receiver load coil).

We have modeled the entire inductive link of the proposed design (Tx and Rx units) and a realistic human body using ANSYS HFSS software to optimize the system. This model

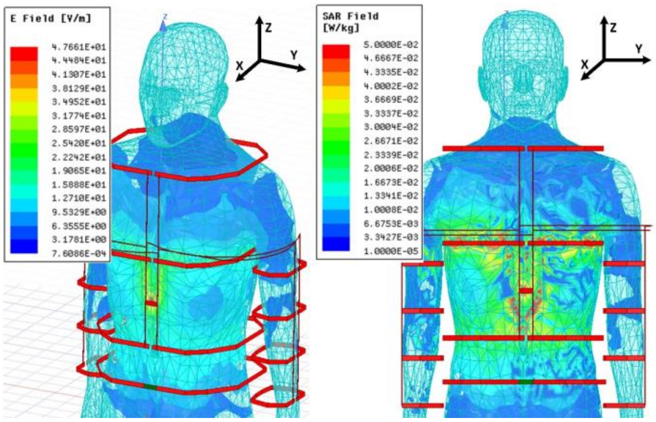

(a) (b)

Fig. 4. The HFSS 3D model and simulation results of the proposed cluster-based inductive link (all resonators are in parallel configuration) wrapped around the human body model; including (a) the E-field generated by the resonators, and (b) the average-SAR simulation results with 1 W power input.

includes all the resonators (inductors and capacitors) of the cluster, paralleled with thin wires. We have determined that a flat wire (copper foil) with 9 mm width and 0.1 mm thickness provides a higher coil quality factor and self-resonance frequency (SRF) comparing with AWG wires for implementing the Tx coil and resonators in parallel configuration. In our simulation, we have changed the gap between the resonators to find the optimum coupling coefficient (minimum achievable S_{11}) for maximizing the uniformity of the PTE and PDL. Fig. 3a shows the coupling coefficients as a function of the distance between an Rx coil and two adjacent resonators in parallel configuration for different gaps between those adjacent resonators at the central body. Considering the requirements of the target application (PTE, PDL, uniformity, etc.), we chose the gaps between the resonators using the results presented in Fig. 3a. The insets of Fig. 3a show the HFSS model developed to optimize the design. We have considered two different sizes of resonators in the cluster in our model: 1) the chest and waist resonators, shown in Fig 3a, and 2) forearm resonators, shown in Fig 3b. The HFSS simulation results presented in Fig. 3b indicate the coupling coefficients as a function of the distance between an Rx coil and two adjacent resonators in parallel configuration for different gaps between those adjacent resonators at the forearm area. Based on the simulation results shown in Fig. 3, the coupling coefficient decreases with the increase of distance between two resonators. The optimal separations for the torso and forearm resonators are determined to be 200 mm and 100 mm, respectively.

The HFSS 3D model and simulation results of the E-field generated by the resonators are presented in Fig. 4a. This simulation includes the human body model and the entire inductive link of the proposed design, in which all resonators of the cluster are paralleled. This figure indicates the uniformity of the electromagnetic field inside the human body. Eleven resonators (worst-case scenario) are used to cover the entire upper human body area for evaluating the Specific Absorption Rate (SAR). The SAR measures the radio-frequency energy absorbed (per unit mass) by the human body when exposed to an electromagnetic field. The average-SAR simulation result is shown in Fig. 4b, while the

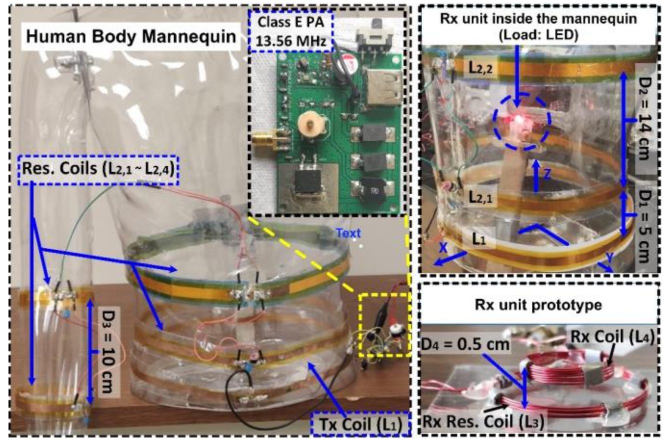

(a) (b)

Fig. 5. (a) The implemented prototype of the proposed design with one Tx coil and four resonators in parallel configuration, wrapped around a human body mannequin, indicating the implemented Class E Power Amplifier, and (b) the Rx coil unit (with wirelessly powered LED) and its location inside the human body mannequin.

TABLE 1. SPECIFICATIONS OF THE IMPLEMENTED COILS AT 13.56 MHZ.

Parameter	*Tx Coil (L_1)*	*Res. Coil ($L_{2,1}$/ $L_{2,2}$)*	*Hand Res. Coil ($L_{2,3}$/ $L_{2,4}$)*	*Rx Res. Coil (L_3)/ Rx Coil (L_4)*
Inductance, L (μH)	0.65	0.74/0.73	0.24/0.25	1.76/1.54
Quality Factor, Q	128	164/185	313/303	124/88
Outer Diameter, do (mm)	320*240	320*240	100*80	30/20
Inner Diameter, di (mm)	do-0.1	do-0.1	do-0.1	do-0.4
Coil Widths/ Diameter, W (μm)	900	900	900	400
Spacing, S (μm)	-	-	-	100±50
Turns (N)	1	1	1	5/7
Coil (Copper) Type	Foil	Foil	Foil	26AWG
Intermediate Distance, D (cm)	D_1 = 5 (L_1/ $L_{2,1}$)	D_2 = 14 ($L_{2,1}$/$L_{2,2}$)	D_3 = 10 ($L_{2,3}$/$L_{2,4}$)	D_4 = 0.5 (L_3/L_4)

input power of the system was set to be 1 W. The maximum level of the simulated average-SAR equals 0.05 W/kg, which is well below the standard of 1.6 W/kg [11].

III. EXPERIMENTAL RESULTS

We have used flexible copper foil to implement the Tx coil and resonators (one-turn coils with a 9.00 mm width using 3M RF EMI Shielding Tape). The thickness of the utilized copper foil equals 0.1 mm, and we have covered the coils with Kapton adhesive tape (both sides) for electrical isolation and protecting the copper foil. The implemented prototype (Tx coil and resonators in parallel configuration) is assembled on a human mannequin to characterize the performance of the design in the 3D space of the human body model. Fig. 5a shows the implemented prototype of the proposed design consists of the Tx coil and four resonators in parallel configuration (wrapped around a human mannequin). The inset of Fig. 5a indicates the implemented Class E Power Amplifier, developed to generate the 13.56 MHz power signal. Fig. 5b shows the Rx unit (L_3 and L_4), which is wirelessly powered inside the mannequin. An LED is used as

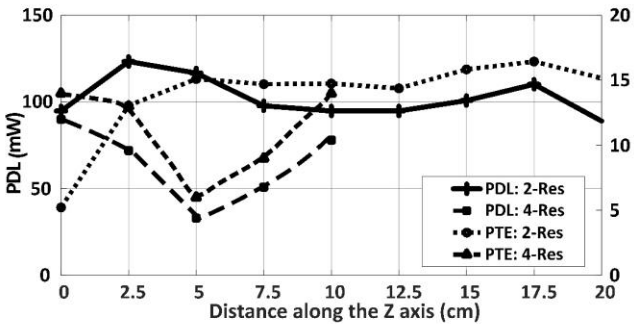

Fig. 6. Measured PDL and PTE while sweeping the Rx unit location along Z-axis for the scenarios of having only two resonators in parallel configuration in the system around the body torso and four resonators in the system (two resonators around the body torso and two resonators around the forearm area).

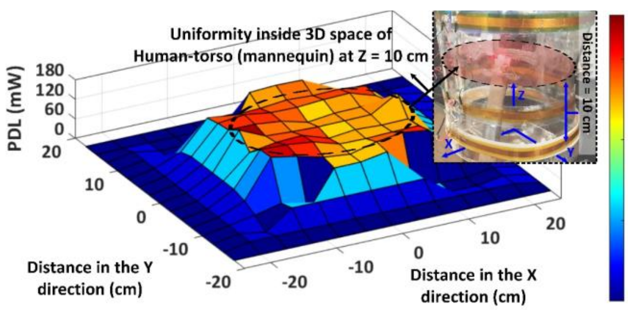

Fig. 7. The measured PDL at the surface between two resonators by sweeping the Rx unit along the X and Y axes inside and outside of the human mannequin.

an Rx load to visualize the delivered power. The specifications of the inductors (L_1, $L_{2,i}$, L_3, and L_4) of the implemented prototype are presented in Table 1.

Fig. 6 shows the measured PTE and PDL as a function of the separation distance between the Rx unit and Tx resonators while the Rx unit is at the center of the paralleled Tx resonators and swept along the Z-axis. In this prototype, the gap between the resonators at the central body and forearm area equal 14 cm and 10 cm, respectively. We have characterized the performance of the prototype with (N=4) and without (N=2) the forearm resonators regarding the PTE and PDL. We have calculated PTE by measuring the transmission coefficient, S_{21}, of the link using (2).

$$PTE = |S_{21}|^2 * 100\ \% \qquad (2)$$

We have used a two-port vector network analyzer (VNA) to measure the S_{21}, where Tx coil, L_1, and receiver load coil, L_4, are directly connected to the VNA's ports. For this measurement, $R_S= R_L= 50\ \Omega$. We have calculated PDL with equation (3) by measuring the voltage (V_{p-p}) across the Rx load, $R_L= 220\ \Omega$, while the voltage across the PA has set to be 10V DC.

$$PDL = (V_{p-p} / 2)^2 / 2 * R_L \qquad (3)$$

Fig. 6 indicates the measured uniformity of PDL and PTE in the body torso region along the Z-axis. The PDL varies from 95 mW to 123 mW, and PTE remains constant at around 15% in the area between 2.5 cm (from the Tx coil) and 20 cm (the second resonator location). The measured PDL in the forearm area (along Z-axis) varies between 33 mW and 90 mW, while the average PTE equals 10% in the same area.

Fig. 7 shows the measured PDL in the central body area between two resonators in parallel configuration (10 cm above Tx coil (Z=10), while the location of the Rx unit is swept horizontally along the X and Y directions. The inset of Fig. 7 shows the XY plane (an elliptic shape with a dashed line) inside the human mannequin, where the PDL values are measured. The measured results demonstrate uniform PDL inside the mannequin and a sharp drop in the PDL outside the mannequin/resonators. Figs. 6 and 7 together validate the capability of the proposed design in powering the Rx unit in the 3D space inside the body or area between the resonators in parallel configuration, wirelessly.

IV. Conclusion

A novel multi-coil inductive link configuration with parallel resonators is proposed for powering implantable devices in the 3D space of the human body. The HFSS model of the proposed WPT inductive link is developed to optimize the design to achieve uniform PDL and PTE inside the human body and evaluate the SAR level regarding the body safety concerns. The proposed design is implemented and assembled on a human mannequin. The implemented prototype consists of a Class E PA, a Tx coil, a cluster of four resonators, and an Rx unit. Homogeneous power is delivered to the Rx unit, wirelessly, everywhere inside the 3D space of the human body model. The PDL and PTE of the design are measured >120 mW and 15% inside the central part of the body model, respectively. A PTE of 14% is measured at the forearm area of the human mannequins while delivering 90 mW to the Rx unit.

V. References

[1] S.Y.R. Hui, W. Zhong, and C.K. Lee, "A critical review of recent progress in mid-Range wireless power transfer," *IEEE Trans. on Power Electronics*, vol. 29, no. 9, pp. 4500-4511, Sep. 2014.

[2] S.A. Mirbozorgi, E. Maghsoudloo, H. Bahrami, M. Sawan, and B. Gosselin, "Multi-resonator arrays for smart wireless power distribution: comparison with experimental assessment," *IET Power Electronics*, vol. 13, no. 18, pp. 4183 – 4193, Dec. 2020.

[3] S.A. Mirbozorgi, H. Bahrami, M. Sawan, and B. Gosselin, "A smart cage with uniform wireless power distribution in 3D for enabling long-term experiments with freely moving animals," *IEEE Trans. on Biomedical Circuits and Systems*, vol. 10, no. 2, pp. 424-434, Apr. 2016.

[4] K. Agarwal, R. Jegadeesan, Y.X. Guo, and N.V. Thakor, "Wireless power transfer strategies for implantable bioelectronics," *IEEE Reviews in Biomedical Engineering*, vol. 10, pp. 136-161, Mar. 2017.

[5] J.C. Olivares-Galvan, *et al*., "Wireless power transfer: Literature survey," *IEEE International Autumn Meeting on Power Electronics and Computing (ROPEC),* Morelia, Mexico, pp. 1-7, Nov. 2013.

[6] E.M. Knavel, and C.L. Brace, "Tumor ablation: common modalities and general practices," *Techniques in vascular and interventional radiology*, vol. 16, no. 4, pp.192-200, Dec. 2013.

[7] R.M. Gore, *et al*., "That liver lesion on MDCT in the oncology patient: Is it important?," *Cancer Imaging*, vol. 12, no. 2, pp. 373–384, 2012.

[8] K. Na, H. Jang, H. Ma, and F. Bien, "Tracking optimal efficiency of magnetic resonance wireless power transfer system for biomedical capsule endoscopy," *IEEE Trans. on Microwave Theory and Techniques*, vol. 63, no. 1, pp. 295-304, Jan. 2015.

[9] S.A. Mirbozorgi, H. Bahrami, M. Sawan, and B. Gosselin, "A smart multicoil inductively coupled array for wireless power transmission," *IEEE Trans. on Ind. Elec.*, vol. 61, no. 11, pp. 6061-6070, Nov. 2014.

[10] D. Ahn and M. Ghovanloo, "Optimal design of wireless power transmission links for millimeter-sized biomedical implants," *IEEE Trans. on Biom. Cir. and Sys.*, vol. 10, no. 1, pp. 125-137, Feb. 2016.

[11] A. Christ, *et al*., "Evaluation of wireless resonant power transfer Systems with human electromagnetic exposure limits," *IEEE Trans. on Electromagnetic Compatibility*, vol. 55, no. 2, pp. 265-274, Apr. 2013.